



# HARD CLUSTERING OF ESN DYNAMICS USING CONCEPTORS

Bachelor's Project Thesis

Joris Peters, s4001109, j.peters.13@student.rug.nl,

Supervisors: G.Pourcel & Prof Dr H. Jaeger

**Abstract:** For data analysis, explainability, and more, it can be of interest to identify groups and hierarchies within the activity dynamics of recurrent neural networks (RNNs). Using conceptors to represent RNN dynamics, this study aims to cluster the dynamics of Echo State Networks (ESNs), a variant of RNNs. Conceptors were computed from the ESN-response to phoneme recordings of the TIMIT dataset. These conceptors were then used to perform phoneme classification with evidences (supervised), clustering with an adaptation of K-means (unsupervised), and hierarchical clustering with average linkage (partly supervised). Conceptor-based phoneme classification reached a reasonable [In addition to classification, I show that conceptors may be used for clustering into groups and hierarchies.] accuracy and clustering produced groups and hierarchies that resemble existing phonetical taxonomies. I conclude that conceptors are well-suited to classifying and clustering ESN-dynamics and the time-series that induced these dynamics.

## 1 Introduction

Topic: Use conceptors to identify discrete symbols (clusters) within the dynamics of Echo State Networks (when driven with speech samples).

### 1.1 Background

All models are wrong, but some are useful. On the one hand, biological and artificial cognitive agents benefit from internal models of their environments; These models form the playing fields to various cognitive functions like reasoning, creativity, attention, memory, and language. On the other hand, the usefulness of the resulting cognitive functions depends, to some degree, on the adequacy of the underlying models. For instance, in recall tasks, a well-suited task model that chunks together related information (like adjacent numbers (Miller, 1956) or chess pieces (Chase and Simon, 1973)) can aid its short memorization. Likewise, in artificial agents, a good world model can often simplify the task (...).

Traditional cognitive science frames the nature of cognitive models as fundamentally symbolic. The hypothesis of Newell and Simon (1975) that humans, computers, and any other system capable of intelligence must be a physical symbol system,

one that performs operations on symbols, has been widely adopted. Symbols are entities that represent other entities. Human speech may exemplify the symbolic nature of our cognitive models. Phonemes are the mental representations of phones, the smallest still distinguishable units of speech sound. For example, the phoneme /t/ is a symbol of the English-proficient mind and the mental representation of the phones [t<sup>h</sup>], [t], and [r]\*, each of which encompasses a subset of speech sounds. The phones that a phoneme represents are its *allophones*. Communication through speech is possible, among many other factors, for the speech models of the communicators coincide; The models of English speakers generally feature the same 44 phonemes representing the same set of phones with some variability across dialects. Note that phonemes are language specific; Every language uses a different set of symbols to represent its particular speech sounds. Thus, cognition seems to rely on symbolic models.

Cognitive neuroscience attempts to explain how these cognitive symbols arise in sub-symbolic brains. From a sub-symbolic perspective, the brain is a net-

---

\*Phonemes are broadly transcribed using a slanted bracket. Phones are narrowly transcribed by a square bracket. Phonic transcriptions will be written using the International Phonetic Alphabet (IPA).

work of neurons. When this dynamical system is stimulated, for example, by sensory inputs, patterns of neural firing result. These firing patterns may be considered symbols if they are associated with a specific entity. Symbol acquisition, then, is the process of reinforcing these firing patterns (through Hebbian learning) face to the repeated exposure to instances of the referenced entity. For example, when a child is first exposed to speech, every sound signal will trigger an arbitrary firing pattern. As the child repeatedly hears the phones  $[t^h]$ ,  $[t]$ , and  $[r]$  in similar linguistic contexts, a single pattern of neural firing becomes associated with them. This pattern corresponds to the cognitive symbol, the phoneme,  $/t/$ . After symbol acquisition, the pattern is no longer tied to any specific instance but represents a whole subset among the possible speech sounds and sensory experiences in general). Notably, children learn to distinguish phonemes without external supervision; No explicit instructions are needed let alone possible since only later in development do phonemes become the building blocks of words and enable the understanding and production of language Maye and Gerken (2000). So, symbols correspond to sub-symbolic firing patterns acquired through unsupervised learning.

The field of artificial intelligence (AI) has sought to bridge between its symbolic and sub-symbolic representations. One such bridge is being built between Echo State Networks (ESNs) that are, like the human brain, networks of sub-symbolic units (neurons) and *conceptors* that offer a symbolic representation of the sub-symbolic firing patterns. I will proceed by introducing ESNs and then conceptors taking inspiration from Jaeger (2014). On the sub-symbolic end, ESNs are a type of recurrent neural network. As such, they implement a dynamical system; Their internal states are a function of time. This time-extended activity relies on cyclic connections to introduce memory into the system and enable the processing of time series like speech. However, ESNs distinguish themselves from other RNNs by their large size (many internal neurons), low density (low connections-to-neurons ratio), and random and untrained internal- and input weights (Yildiz, Jaeger, and Kiebel, 2012). Given these features, ESNs can have a capacity for performing a high-dimensional non-linear expansion of their input signals, that, under the right circumstances, uniquely *echo* of these inputs, paralleling how a brain may transform sen-

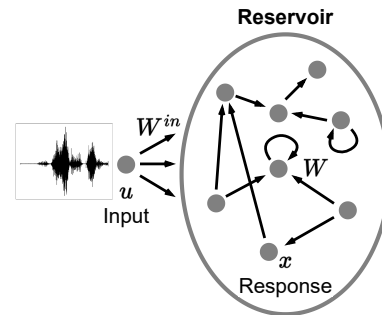


**Figure 1.1:** Sketch of an ESN driven with an input signal. State vector  $x$  is a high-dimensional response to the input signal  $u$ .

sory inputs into characteristic neural firing patterns. Figure 1.1 depicts a typical ESN as it is driven by an input sequence  $u$ , possibly a speech sample, and elicits a high-dimensional response  $x$ , the sequence of internal states of the ESN’s reservoir. An output layer is sometimes added to ESNs for (re)productive purposes but omitted here since only the internal states of the network will be of interest for the current study as will become apparent shortly.

On the symbolic end, conceptors offer a symbolic representation of the sub-symbolic activity patterns within neural networks like ESNs. A conceptor is a positive semi-definite matrix that can be derived from any set of network states like the state sequence  $x$ . Their mathematical properties (Section 1.5.2) allow conceptors to, i.e., recognize, control, compare, combine, and logically evaluate patterns of network activities. Thereby, using conceptors, groups of ESN activities are considered as entities **[(possibly discrete and semantic)]** similar to how neural firing patterns of the brain were considered symbols by cognitive neuroscience. Thus, conceptors can be used as lenses on the dynamics of ESNs; lenses that open up a variety of symbolic mechanisms.

A common use-case of conceptors with ESNs has been supervised time series classification (Jaeger, 2014). An instance of this method will be outlined in Experiment 2.4, but the guiding idea is the following. Under the echo state property (ESP), an ESN responds uniquely to its inputs; i.e., there is a functional relationship between inputs and responses **[Why is it not bijective?]**. More concretely, with this functional relationship between

inputs and responses, the responses can be seen as high-dimensional embedding of the input. Hence, any label assigned to a reservoir response is taken to equally apply to the input sequence that induced that response. To train the classifier, one captures the reservoir responses of each class using a conceptor. To classify, the new response is assigned the class whose conceptor indicates the highest similarity [or correlation?] to the previously seen responses of the class. Jaeger, Lukoševičius, Popovici, and Siewert (2007) demonstrated this method in speaker recognition on the *Japanese Vowels* dataset to a perfect accuracy, a result that promisingly exceeded several previous attempts. [Describe the advantages of this classification method.] Building on this experiment, Vlegels (2022) showed that competitive accuracies in the classification of non-stationary time-series may be achieved using several variations of this methods. Moreover, Chatterji (2022) adapted the method to time-series *recognition*. The difference between classification and recognition is that the former estimate the class of pre-segmented signals (one label per segment), whereas the latter estimates the class present within unsegmented signals (multiple labels per signal over time) (Lopes and Perdigao, 2011). Concretely, Chatterji (2022) demonstrated their method on the recognition of phonemes on the TIMIT Acoustic-Phonetic Continuous Speech Corpus (TIMIT), the dataset also used in the current study. Concluding, in the supervised tasks of time series classification and recognition, the classes of interest are given, but they may not always be.

Unsupervised learning tasks typically involve analyzing the structure of data without given classes or labels. For example, one may seek to identify important clusters (groups), hierarchies of clusters, axes, or relationships among a set of data points. In the following cases, conceptors were used to identify initially unknown structures or relationships among neural network state clouds for explainability and data analysis. Bricman, Jaeger, and van Rij-Tange (2022) used conceptors for neural network explainability. The developed technique, Nested State Cloud, extracts a knowledge graph from the latent space encodings of a set of 100 symbols (e.g., "apple"). Each symbol encompassed multiple instances, contexts in which they appear (e.g., "The apple fell."), all of which had different embeddings. Conceptors served as a compact representation of each symbol's embeddings and allowed them to be seman-

tically related in the graph. Similarly, Mossakowski, Diaconescu, and Glauer (2019) used conceptors to represent and then organize classes of network states. This time, the symbols (i.e., classes) were Japanese speakers, and the network states were an ESN's responses to their speech samples. Using the fuzzy generalization of the Löwner ordering as a dissimilarity function on the speaker-specific conceptors, the symbols were organized in a tree by hierarchical agglomerative clustering. The authors mention the potential application in classification, but whether the resulting hierarchy truly coincided with any features of speakers like dialectal groups remained unknown. These studies analyze structures between classes of reservoir states, but this means that they, like the supervised classification algorithm, start from pre-established symbols. I shall refer to these as *above-symbol structures*, for they are at a level of abstraction above that of symbols.

## 1.2 Motivation

A significant challenge and the main aim of this study lies in unsupervised symbol identification<sup>†</sup>. The motivation for analyzing such *below-symbol structures* is the move toward more autonomous cognitive agency with applications in, for instance, computational creativity. Concretely, in the context of ESNs, the question arises of how to determine which network state instances should be included within each conceptor, that is, which patterns of network activity should be treated as the same symbol. It is relevant for several reasons. Firstly, unsupervised symbol identification is a step toward more general cognitive agency. Models are often fed with a priori information on their task to improve performance; for instance, the dataset for training a speech recognition model may feature additional phonemic transcriptions. These will be used to form the model's task representation. However, there often is little basis to presume that, for any given task, the known domain model is optimal, resonating with the idea that all models are wrong to different degrees. Moreover, for yet unsolved tasks, the inability to autonomously identify relevant symbols may form a ceiling to machine cognition. This need for autonomy is analogous to the earlier example of

<sup>†</sup>Symbol identification is distinct from acquisition since no learning is involved.

how children need to learn to distinguish phonemes due to, or rather in spite of, the lack of explicit instruction or supervision.

Secondly, computational creativity, in particular, may require the unsupervised generation of new symbols. According to Boden (2004), the most advanced type of creativity involves transforming an existing conceptual space. For example, some groundbreaking scientific discoveries may not be reachable via the mere exploration of existing theories (the current conceptual space) but may require a shift in the problem representation. Similarly, Douglas Hofstadter models creativity as an ability to form and alter symbols. Thus, without the capability to discover new symbolic representations, the creative agent might find itself quite limited, capable of optimizing, but unable to redefine the problem space itself. Regarding analogy-making, a core feature of human creativity, Hofstadter’s Copycat model thereof relies on the fluidity of symbolic representations. Therefore, potential improvements in the available symbols could enhance analogical reasoning potential and, by extension, creative potential.

The identification of both below- and above-symbol structures resembles classical clustering tasks. Clustering refers to the unsupervised task of organizing a data set into groups, or *clusters*, such that instances within the same cluster are more similar to each other than to those of other clusters. This similarity may be determined by a dissimilarity measure like the Euclidean distance. Clustering could play a significant role in finding below-symbol structures relevant to unsupervised symbol identification. By feeding the states of a neural network into a clustering algorithm, they can be grouped into clusters, each of which can then be treated as a symbol with the cluster members being the representations of that symbol. The analogy holds, for similarity is expected among states of the same symbol and dissimilarity between states of different symbols. Conceptors may serve to represent and evaluate the clusters. Conceptors can compactly represent and compare sets of network states and thereby act as centroids, i.e., exemplar-based representations of the symbols Bricman et al. (2022). Hence, the process of unsupervised symbol identification will be seen as a form of clustering, where each cluster corresponds to a symbol and is represented by a conceptor. Similarly, clustering algorithms seem equally applicable to the analy-

sis of above-symbol structures by pre-grouping the network states by symbol according to a priori memberships.

A final motivation is to extend the use cases of conceptors to time series clustering. Reiterating, conceptor-based time series classification was achieved by classifying an ESN’s responses to the time series. Similarly, clusters found among ESN dynamics may coincide with relevant clusters among the time series that underlie these dynamics. This relationship will prove useful in extrinsically evaluating the clusters. Moreover, the formalism of conceptors would thus be extended to time series clustering.

**RQ** Concluding, this study explores conceptor-based, unsupervised, options for identifying symbols within the sub-symbolic dynamics of ESNs (the responses to input time series). Therefore, it investigates the question of whether meaningful clusters and hierarchies can be identified among ESN state sequences. These structures are considered meaningful if they coincide with domain-relevant features of the corresponding inputs.

### 1.3 Justification of Experiments

I take inspiration from two classical hard clustering algorithms, K-means and hierarchical agglomerative clustering (HAC). Hard clustering assigns each data point to one, and only one, cluster, enforcing a clear separation between clusters. In contrast, soft clustering, like that of Bricman et al. (2022), assigns data points a level of membership for each cluster, allowing for overlap between clusters. I assumed, in the spirit of traditional symbolic representation theory, hard clustering to be the better fit for the endeavor of automated symbol identification using symbols to represent discrete, separated entities instead of multiple entities to varying degrees. ESN dynamics will be hard-clustered by adapting K-means and HAC, two well-known hard clustering algorithms with guaranteed convergence. K-means partitions data into a number of non-overlapping clusters and will be used to group below-symbol instances into symbolic groups. Importantly, traditional K-means can cluster  $N$  data points within  $O(N)$  enabling its use on larger data sets. Meanwhile, HAC returns a hierarchy of clusters and will be used to analyze above-symbol structures among pre-existing symbols. HAC requires  $O(N^2)$  with

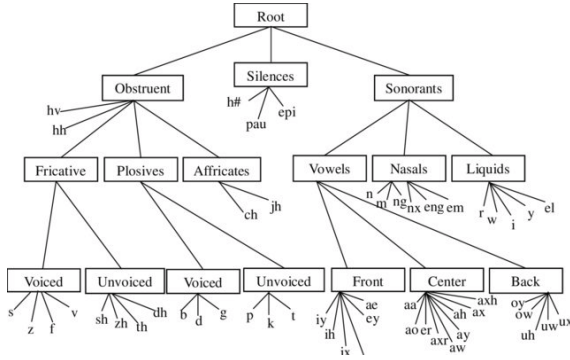


**Figure 1.2: A taxonomy of all phones present in TIMIT Pfeifer and Balik (2011)**

optimal implementation. Both algorithms have previously been used for time series clustering by [...]. However, while ESN state sequences are time series, it is unclear whether the previous methods are suited to the clustering of high-dimensional non-linear dynamics. Moreover, previous time series clustering algorithms have scaled badly with long, potentially infinite, time series, were often offline (fail to adapt as new data points), or struggled to handle variable length time series, a limitation mediocly solved using Dynamic Time Warping. These shortcomings were equally menacing time series *classification* algorithms but were resolved by use of conceptors; the similarity in methods gives hope to similarly resolve them in conceptor-based time series *clustering*.

The developed methods will be demonstrated on phonemic speech recordings. As mentioned, Phonetics – the branch of linguistics concerned with speech – groups speech sounds into phones (sound units) and phones into phonemes (symbols); yet, further above-symbol organizations exist. For example, Figure 1.2 depicts a possible taxonomy of the phonemes present in the TIMIT corpus which contains clusters like vowels and nasals<sup>‡</sup>.

The availability of these phonetic systems makes phoneme recordings a good domain for evaluating clustering algorithms. On the one hand, these phonemic classes and taxonomies can be used as ground truth clusterings to determine the performance of the developed clustering algorithms. On the other hand, the results from this study may provide an

empirical verification or falsification of phonetic theory; whereas the groups and taxonomies of phones were largely developed based on their articulatory features, the following clustering Experiments will investigate whether these groups can be found on a purely acoustic basis. [Phonemes clustering literature on TIMIT (reference to methods to avoid redundancy)] [transition]

For clustering ESN responses to phoneme recordings, the ESN must be suited for the task. The following assumption affects the experimental design; Given an ESN, the more accurately a conceptor-based classifier can distinguish activity groups, the better these classes can be retrieved by an unsupervised clustering algorithm. The classification and clustering performances seem correlated because, for many hyperparameters like the aperture and spectral radius, a sweet spot seems to exist, where the ESN’s signal-to-noise ratio is maximized and where the network is neither over- nor under-excited, that can be determined independent of the application in clustering or classification. Thus, I assume that tailoring the ESN to the TIMIT data and classification task will improve clustering on the same data. The hyperparameters were optimized in Experiment 1 on time series classification. Moreover, performing the classification task in Experiment 1 has the positive side-effect of demonstrating the application of conceptors to the phoneme classification on the TIMIT dataset. The following classification method builds on that of Jaeger (2014). To my knowledge, the currently highest accuracy of 78.4% for phoneme classification on TIMIT’s test set was achieved using fixed-sized kernel logistic regression [Karsmakers, Pelckmans, Suykens, and hamme (2007) mentioned in Lopes and Perdigao (2011)].

## 1.4 Conclusion

Concluding, this study aims to identify groups (below-symbol) and hierarchies (below-symbol) among ESN states. The next section will provide a more formal introduction to ESNs, conceptors, and the adapted clustering algorithms. Experiment 1 will be a classification task used to tune the hyperparameters to be used in Experiments 2 and 3. In Experiment 2, K-means will be adapted to group the ESN responses to individual phoneme recordings. Experiment 3 will attempt to distill hierarchies of pre-grouped ESN responses.

<sup>‡</sup>The TIMIT labels, also shown in Figure 1.2 and listed in Table A.1, are from IPA, although not written in Greek letters. The translation keys are given in the documentation.

## 1.5 Formal Definitions

The following sections on ESNs and conceptors were inspired by the detailed report Jaeger (2014). For an index of some of the mathematical notations used throughout the paper, please refer to Appendix B.

### 1.5.1 Echo State Networks

Let us formalize an example ESN like the one from Figure 1.1. Let  $N$  be the number of internal neurons. As mentioned,  $N$  will typically be large relative to the dimensionality  $d$  of the input. The input weight matrix  $W^{in} \in \mathbb{R}^{N \times d}$ , the bias vector  $b \in \mathbb{R}^N$ , and the internal weight matrix  $W \in \mathbb{R}^{N \times N}$  are randomly initialized, the latter of which will typically contain many zeros to implement the internal sparsity of the reservoir. When driven by a discrete time series input  $u$  of length  $L$ , the ESN elicits a response, the internal state sequence  $x$  of dimensionality  $N$  and of the same length as the input. The ESN’s update equation is that of classical discrete-time RNNs:

$$x(n+1) = \tanh(Wx(n) + W^{in}u(n+1) + b), \quad (1.1)$$

where  $x(n)$  and  $u(n)$  are the internal reservoir state and input column vectors at time step  $n$  and  $\tanh$  is the hyperbolic tangent. We observe that any ESN state depends on the current input and the ESN’s previous internal state. Indeed, the response  $x$  is a high-dimensional non-linear expansion of the input since  $N \gg d$  and  $\tanh$  is applied. For later convenience, we define function  $r$  from the set of input sequences to the set of response sequences where  $r(u)$  is the response that results from driving the ESN with  $u$ . The used ESN and the parameters will be clear from the context where  $r$  is used.

### 1.5.2 Conceptors

**Definition and Intuition** Given any sequence of network states  $x = (x(1), \dots, x(L))$  that may have arisen from running the above ESN <sup>§</sup>, the conceptor matrix  $C$  computed from  $x$  minimizes the following

<sup>§</sup>We consider *sequences* of network states for practicality, but they can be thought of as *sets* because their states need not necessarily be ordered; any ordinal information is lost during the computation of conceptors. Neither do the states need necessarily stem from the same ESN run.

loss function  $\mathcal{L}$ :

$$\begin{aligned} \mathcal{L}(C|x, \alpha) &= \sum_{n=1}^L \|x(n) - Cx(n)\|^2 / L + \alpha^{-2} \|C\|^2 \\ C &= \arg \min_C \mathcal{L}(C|x, \alpha), \end{aligned} \quad (1.2)$$

where  $\alpha \geq 0$  is the conceptor’s aperture (further explained below). The conceptor  $C$  that minimizes  $\mathcal{L}(C|x, \alpha)$  may be analytically computed via the following procedure:

1. Concatenate the states in  $x$  column-wise in an  $N \times L$  collection matrix  $X = [x(1)|\dots|x(L)]$ .
2. Compute the correlation matrix  $R = XX'/N \approx \text{corr}(X)$ .
3. Obtain the conceptor  $C(R, \alpha) = R(R + \alpha^{-2}I)^{-1}$  with  $N \times N$  identity matrix  $I$ .

To provide some intuition, conceptors can be considered ’fingerprint’ of the activity of [a] network’ over a period of time (Jaeger, 2014). This potential for conceptors to uniquely identify or fingerprint a sequence of states is reflected in its loss function. When minimizing  $\mathcal{L}$ , the term  $\|x(n) - Cx(n)\|^2$  nudges  $C$  toward realizing an identity mapping for the states  $x(n)$ . However, the regularization term  $\alpha^{-2}\|C\|^2$  attaches a cost to the magnitude of its entries, limiting the numerical resources available to realize this identity mapping. Thus, the conceptor is drawn away from the identity matrix toward the zero matrix, especially on those axes that can account for little of the variance of  $x$ , i.e., where the minimization of  $\|x(n) - Cx(n)\|^2$  is less beneficial. The amount of regularization applied to the conceptor depends on its aperture  $\alpha$ . The higher the aperture, the closer the resulting conceptor maps all the members of  $x$  to themselves. The lower the aperture, the more selective the conceptor becomes, realizing a ’good’ identity mapping only along the important axes that explain most of the sequence’s variance.

A geometric perspective might extend this intuition. The reservoir states being a point cloud in state space  $(0, 1)^N$ , their conceptor can be represented as a hyperellipsoid of a similar shape as the point cloud but constrained to the unit circle of  $\mathbb{R}^N$ . The directions and lengths of the hyperellipsoid’s

axes are given by the singular vectors and values of the conceptor, respectively, and "represent the principle components of the state cloud" (Vlegels, 2022). However, the shape of the hyperellipsoid slightly deviates from that of the point cloud as the regularization *squashes* it along its shorter axes. With a low aperture, the hyperellipsoid would be very squashed, extended only along a few main axes. With a large aperture, the conceptor would be a little squashed and approach the unit hypersphere.

This squashing in space may be seen as a spatial compression as it systematically reduces the variance of the point cloud along its less important axes. Furthermore, conceptors are a temporal compression of ESN state sequences. Mapping sequences of vectors in state-space to conceptor-space turns variable-length objects into constant-sized objects. When the state sequence is a time series, this mapping removes the temporal dimension, whence it may be seen as a temporal compression. **[Is there a better way to describe this compression?]**

**Conceptor operations** The following section describes several useful operations on conceptors some of which illustrate their symbolic nature. [Elaborate]

**Similarity function** Conceptors may be used to compute the similarities of state sequences. If  $C_a$  and  $C_b$  be the conceptors derived from the two sequences of states to be compared, their similarity may be defined as:

$$\text{Sim}(C_a, C_b) = \frac{|(S_a)^{1/2}(U_a)'(U_b)(S_b)^{1/2}|^2}{|\text{diag}(S_a)||\text{diag}(S_b)|}, \quad (1.3)$$

where  $U_a S_a (U_a)'$  is the SVD of  $C_a$  and  $U_b S_b (U_b)'$  is the SVD of  $C_b$ . It is a function of the squared cosine similarity of the conceptors that measures the angular alignment between all pairings of singular vectors of the two conceptors weighted by the corresponding singular values.

**Aperture** The aperture of a conceptor can be set during its computation or when given a pre-computed conceptor  $C$  **[Is it okay to use the name 'C' to refer to other conceptors than this one. Or do I need to name every object differently e.g.,  $C_2$ .]**, its aperture can still be adapted by any factor of  $\gamma > 0$  using the aperture-

adaptation function  $\varphi$  that returns the aperture-adapted conceptor  $C_{new}$ :

$$C_{new} = \varphi(C, \gamma) = C(C + \gamma^{-2}(I - C))^{-1} \quad (1.4)$$

**Logical Operations on Conceptors** Several logical operations have been meaningfully defined on conceptors. Given the arbitrary conceptors  $C$  and  $B$ , we have the following definitions and semantics:

#### 1. Negation ( $\neg$ )

$$\neg C := I - C \quad (1.5)$$

It returns a conceptor that describes the linear subspace complementary to that of  $C$ .

#### 2. Conjunction ( $\wedge$ )

$$C \wedge B := (P_{R(C) \cap R(B)}(C^\dagger + B^\dagger - I)P_{R(C) \cap R(B)})^\dagger \quad (1.6)$$

See Appendix A.1 for details on the computation of  $P_{R(C) \cap R(B)}$ . It returns a conceptor that describes the intersection of the linear subspaces of  $C$  and  $B$ .

#### 3. Disjunction ( $\vee$ )

$$C \vee B := \neg(\neg C \wedge \neg B), \quad (1.7)$$

by De Morgan's law. It returns a conceptor that describes the union of the linear subspaces of  $C$  and  $B$ .

Although a simpler method for computing conjunction and disjunction exists, that method relies on the inversion of  $B$  and  $C$  and thus fails when  $B$  or  $C$  contain singular values of 0. Such singular values may occur in practice, for example, due to rounding or through the negation of conceptors with unit singular values. Therefore, the above method is recommended whenever the absence of null and unit singular values cannot be ensured.

### 1.5.3 Clustering Algorithms

**K-means** K-means is a clustering algorithm aimed at identifying a set of  $K$  clusters among the input data. A partitioning is better the higher the inter-cluster and the lower the intra-cluster similarities among data points. K-means works by iteratively assigning each data point to the nearest centroid - the mean position of all the data points

in a cluster - and recalculating the centroids based on the newly formed clusters. This process repeats until all centroids converged in their position or a maximum number of iterations is reached. The implementation depends, besides  $K$ , on three components:

1. A *set of points*, typically, in Euclidean space.
2. A *function that provides the centroid of a given cluster*, typically, the mean of the points assigned to the cluster.
3. A *function that provides the distance from a point to a cluster*, typically, the Euclidean distance between the data point and cluster centroid. During the assignment step, points are assigned to their closest cluster minimizing this function. [Generalize to Bregman Divergences according to Banerjee, Merugu, Dhillon, Ghosh, and Lafferty (2005) if applicable]

K-means makes several assumptions about the dataset, which can impact its performance:

- Data distribution: The data points are distributed around their respective centroids in a Gaussian or normal distribution.
- Feature Scaling: The features have the same variance and are equally important. Therefore, the data is often normalized or standardized beforehand.
- Independence of features: The features of the dataset are independent of each other, or equivalently, k-means may not work well with datasets where features are correlated.

**HAC** HAC is a clustering algorithm aimed at identifying a hierarchy of clusters among the input data. HAC works by initializing one cluster per data point and then iteratively merging the two closest clusters until a single cluster or a desired number of clusters is obtained. The result is a hierarchical structure of nested clusters commonly visualized as a dendrogram. Its implementation depends on three components:

1. A *set of points*, typically, in Euclidean space.
2. A *function that provides the distance between two points*, typically, the Euclidean distance between the points.

3. A *function that provides the distance between two clusters*. A common choice is the mean distance between all pairs of points (as defined above) in the two clusters. This variant of HAC is coined average linkage.

## 2 Methods and Results

### 2.1 Dataset

The TIMIT Acoustic-Phonetic Continuous Speech Corpus was chosen as the data source for its diverse and phonetically annotated speech signals. Each of 630 American native speakers (from eight dialect regions and of which 30% were female) read ten sentences – five phonetically-compact, three phonetically-diverse, and two dialect sentences - amounting to a total of 6300 utterances. Each utterance comes with a phonetic transcription that indicates which of 64 phones is uttered at any time of the utterance. Moreover, the corpus is split into a training (73 % of the utterances) and a test set, which were used as such in the experiments (Experiment 3 only uses the training set).

### 2.2 Pre-processing

For all experiments, the following pre-processing steps were performed. The utterances were segmented according to the phonetic transcriptions into  $n = 241225$  segments ( $n_{train} = 177080$  and  $n_{test} = 64145$ ), each a vocalization of one phone (Figure 2.1). From each segment, the first  $d = 14$  Mel Frequency Cepstral Coefficients (MFCCs) were extracted. This representation ought to isolate the information most relevant to speech analysis. To compute the MFCCs, the Librosa Python library (McFee, Raffel, Liang, Ellis, Mcvicar, Battenberg, and Nieto, 2015) was used with one MFCC vector computed every 1 ms from a 2.5 ms long sliding window.

The resulting time series were normalized in amplitude and time. First, the amplitudes varied strongly across the channels [the lowest mean amplitude of an MFCC channel ( $\mu_1 = -593.2$ ) is 24.2 times lower than that of the second lowest channel ( $\mu_4 = -22.4$ )]. To grant each MFCC a similarly strong effect on the ESN dynamics under the identically distributed input weights, each channel was



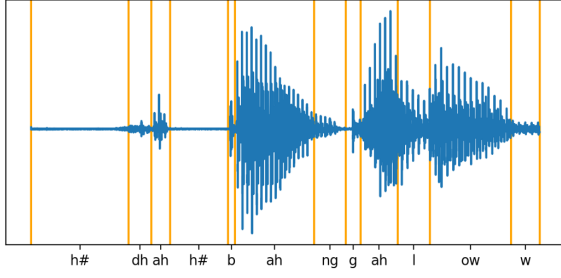


**Figure 2.1:** Example of the twelve first segments of one of the utterances. [will be identified more precisely]

normalized to a range of  $[-0.5, 0.5]$  across all samples. Second, to account for differences in utterance speeds, the series were normalized in time by fitting each channel with a cubic spline and sampling it at  $L = 10$  temporally equidistant points.

Lastly, the phonetic labels (transcriptions)  $p_i$  ( $i = 1, \dots, c$ ) were mapped from the original set of 61 phones to a subset of 39 phonemes  $P$ . Initially proposed by Lee and Hon (1989), this mapping amounts to folding stress-related variations and allophonic variations of phonemes (e.g., /em/ and /m/) into the same classes. The concrete mappings are given in appendix Table A.1 along with the distribution of the resulting classes within the dataset. The mapping serves to reach reasonable classification and clustering performances, render the computations feasible, and make the results comparable to previous studies that also used this mapping [...].

Thus, the resulting data consisted of tuples  $D = \{(s_i, p_i) | i = 1, \dots, c\}$  with MFCC time series  $s_i$ , phone labels  $p_i \in P$ , and the set of phones  $P$  after folding ( $|P| = 39$ ). The ready-made train-test split from TIMIT was used giving  $D_{train}$  and  $D_{test}$  of respective lengths  $n_{train}$  and  $n_{test}$ .

## 2.3 ESN

The following ESN setup was used for all three experiments. It consisted of  $N = 100$  neurons with a connection density of  $r = 10\%$ . The entries of  $W^{in}$  and  $b$  were randomly sampled from a standard normal distribution and rescaled by factors of  $k_{W^{in}} = 1.1$  and  $k_b = 0.6$ , respectively.  $W$  was obtained by random sampling from a standard normal distribution and rescaling the result to a spectral

radius of  $\rho = 2.57$ . The spectral radius of an internal weight matrix like  $W$  is its largest absolute eigenvalue. The larger  $\rho$ , the farther  $W$  transforms the internal state during the state update along its first eigenvector, which tends to lead to a more chaotic behavior.  $\rho$  was adapted by rescaling the old (initial) internal weight matrix  $W_{old}$  to  $W_{new} = \frac{\rho_{new}}{\rho(W_{old})} W_{old}$  where  $W_{new}$  has the desired spectral radius  $\rho_{new}$  instead of the previous  $\rho_{old}$ . [Effects on ESP]

The above hyperparameters were picked by hand based on their effects on the accuracy in Experiment 1, previous research, and resource constraints. All parameters were initially set to the values used in the demonstration experiments of (Jaeger, 2014) (Section 4.1, p. 161).  $N$  was kept as a largest possible value still feasible under the available computational resources. Larger sizes would likely improve performance after adapting the other hyperparameters but may increase the risk for overfitting (Lukoševičius, 2012). The remaining hyperparameters,  $r$ ,  $k_{W^{in}}$ ,  $k_b$ , and  $\rho$ , were adjusted by hand with the objective to maximize the testing accuracy of phoneme classification in Experiment 1. Moreover, automated hyperparameters optimization was attempted but eventually not used due to its large computational cost and slow convergence. Its method and results are in the Appendix.

The resulting ESN was driven independently on each input signal  $s_i$  ( $i = 1, \dots, c$ ) producing the reservoir state sequence  $x_i$  ( $i = 1, \dots, c$ ). Concretely, each run started from the same state  $x(0)$  sampled once from a standard normal distribution not to introduce meaningless between-sample differences while providing the network with an initial excitation. Indeed, using this normally distributed starting state led to a greater testing accuracy in Experiment 1 than when using the null vector as the starting state [Can/Should I just state this without reporting the experiment? And is it tolerated to make such design decisions using the test set given the risk of overfitting?]. The following states  $x_i(t)$  ( $t = 1, \dots, L$ ) were computed via update Equation 1.1 and collected column-wise in  $N \times L$  matrix  $X_i = [x_i(1) | \dots | x_i(L)]$ . Concluding, an ESN response collection matrix  $X_i$  was computed for each training sample .

## 2.4 Experiment 1: Phoneme Classification

### 2.4.1 Objective

The following experiment aimed to classify the pre-processed phoneme recordings. Concretely, the classifier was trained using  $D_{train}$  to assign the correct phoneme label to as many unforeseen speech samples of the test set  $D_{test}$  as possible using only the corresponding ESN responses. The purpose of this experiment was to tune ESN hyperparameters in preparation for the following clustering experiments and to demonstrate conceceptor-based time-series classification on TIMIT.

### 2.4.2 Training

Training amounted to computing one *positive conceceptor*  $C_p^+$  and one *negative conceceptor*  $C_p^-$  from the reservoir states of the phoneme classes  $p \in P$ .<sup>¶</sup> For each class  $p$ , its positive conceceptor  $C_p^+$  models [Decide if *modeled* is the right word, compared to encapsulated, inscribed, represented.] the linear state subspace that ESN states of signals of class  $p$  tend to occupy, and it was computed as follows. Let  $\eta_p$  be the number of training instances of class  $p$ . The state collection matrices corresponding to signals of class  $p$  were concatenated column-wise into a class-level collection matrix  $X_p = [X_1|X_2|\dots|X_{\eta_p}]$  from which  $C_p^+$  was computed with an initial aperture of  $\alpha = 1$  by steps 2 and 3 of the procedure for conceceptor computation. This was repeated for each class to obtain the set of preliminary positive conceptors  $C_{pre}^+ = \{C_p^+ | p \in P\}$ .

**Aperture adaptation** After computing the conceptors in  $C_{pre}^+$  with the initial aperture of  $\alpha = 1$ , their apertures were optimized. First, one new aperture was chosen for all positive conceptors. Here, the goal was to maximize their sensitivity to differences in the underlying ESN dynamics, likely improving their ability to classify the data to come. This sensitivity is reflected by the  $\nabla$ -*criterion*, which measures the magnitude at which the size  $\|C\|^2$  of a conceceptor  $C$  changes with respect to its log aperture – and a change in aperture corresponds to a scaling of the

underlying ESN states (see p. 49 of Jaeger (2014)). Concretely, the  $\nabla$ -*criterion* is defined on a given conceceptor  $C$ , whose aperture is adapted by a factor of  $\gamma$ , and returns the gradient of the Frobenius norm of the aperture-adapted conceceptor with respect to the logarithm of  $\gamma$ <sup>||</sup>:

$$\nabla(C, \gamma) = \frac{d}{d \log(\gamma)} \|\varphi(C, \gamma)\|^2 \quad (2.1)$$

To approximate the optimal aperture, i.e.,  $\gamma_p$ , for each positive conceceptor  $C_p^+$ , 200 candidate values  $\gamma_{candidate}$  in the interval  $[0.001, 500)$  were swept through on a logarithmic scale, for the optimal value was expected on the lower end of the interval. The  $\gamma_{candidate}$  that maximized a numerical approximation of  $\nabla(C_p^+, \gamma_{candidate})$  (with a delta in  $\gamma$  of  $h = 10^{-4}$  [**Does the method for approximating the derivative need further explanation?**]) was taken for  $\gamma_p$ .  $|P| = 39$  values  $\gamma_p$  ( $p \in P$ ) resulted. Finally, the apertures of all positive conceptors were adapted using the mean  $\gamma_{opt} = \frac{1}{|P|} \sum_{p \in P} \gamma_p \approx 133.98$ . Let  $C_{opt}^+$  be the resulting set of aperture-optimized positive conceptors.

The reason for adapting all conceptors to the same aperture instead of adapting each conceceptor with their  $\gamma_p$  is to avoid classification bias. The larger a conceceptor’s trace (the sum of its singular values), the larger the expected *evidence* later used for classifying new sequences [**Should I add the proof to appendix?**]. Thus, if there are differences between the traces of the conceptors, the classifier will be biased toward the classes whose conceptors have greater traces. A similar bias occurs by increasing the expected conceceptor similarity later used for clustering. Since a conceceptor’s trace strongly covaries with its aperture, the latter is used to control the trace [**Do I need a citation, proof, or explanation for this?**]. Equating the apertures between classes helped as first step to approach their traces and debias the classifier.

However, although the conceptors were adapted to the same aperture, some variation in their traces remained as can be seen at  $x = 1$  in Figure 2.2. To remove it, each conceceptor’s trace was adapted to reach a shared target value  $tr_{target} = \bar{tr}$  set to the

<sup>¶</sup>Not the pre-processed speech recordings  $s_i$  ( $i = 1, \dots, \eta_p$ ) are used for classification but the states collected when driving the ESN with them.

<sup>||</sup>In this case,  $\gamma = \alpha_{new}$ , where  $\alpha_{new}$  is the candidate target aperture since  $\gamma = \frac{\alpha_{new}}{\alpha}$  and the current aperture  $\alpha = 1$ .

mean the mean trace among the conceptors:

$$\bar{tr} = \frac{1}{|C^+|} \sum_{C \in C_{opt}^+} \text{tr}(C) \approx 57.23 \quad (2.2)$$

To adapt each conceptor's trace to this target value with an error tolerance of  $\epsilon$  (here,  $\epsilon = 0.01$ ), Algorithm 2.1 was developed. The iterative procedure adapts the conceptor's aperture by a factor of the current trace error ratio until reaching the target trace. This works because, again, trace and aperture covary. We shall call  $\psi(C, tr_{target}, \epsilon)$  the function computed by the algorithm.

---

**Algorithm 2.1** Adapt the trace of a conceptor

---

**Require:**

Conceptor  $C$  whose trace is to be adapted to  $tr_{target}$   
 Target trace  $tr_{target}$   
 Error tolerance  $\epsilon$

**while** TRUE **do**

**if**  $|tr_{target} - tr(C)| < \epsilon$  **then**  
     **break**

**end if**

$\gamma \leftarrow tr/tr(C)$

$C \leftarrow \varphi(C, \gamma)$

**end while**

---

As shown in Figure 2.2 for  $x > 1$ , applying  $\psi(\cdot, \bar{tr}, 0.01)$  to each of the conceptors in  $C_{opt}^+$  normalizes their traces. Thus, via the above two aperture adaptation procedures, the apertures of the conceptors in  $C_{pre}^+$  were optimized and their traces were normalized resulting in the final set of positive conceptors  $C^+$ .

**Negative conceptors** From  $C^+$ , the set of negative conceptors  $C^- = \{C_p^- | p \in P\}$  was computed. Each class' negative conceptor models the linear state subspace that is complementary to the space occupied the states of all other classes. Or, equivalently, it models the subspace that states "from none of the other classes" are expected to occupy. These semantics are reflected in their formal definition:

$$C_p^- = \neg \bigvee \{C_q^+ | q \in P, q \neq p\}, \quad (2.3)$$

where  $\bigvee S$  is the disjunction of the  $|S|$  conceptors in set  $S$  computed by the associative disjunction of

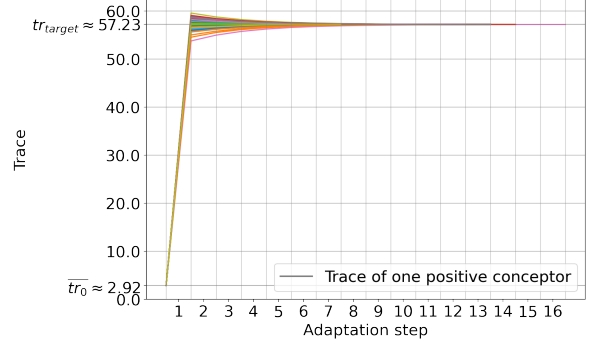


**Figure 2.2:** The traces of the positive conceptors in function of the adaption steps. The first adaptation step 1 is the aperture adaptation based on the  $\nabla$ -criterion. The increase in aperture caused the traces to increase and diverge. The remaining steps ( $x > 1$ ) are the results of normalizing the traces using Algorithm 2.1. Finally, these aperture adaptation steps resulted in an increase of the mean trace from an initial value of  $\bar{tr}_0$  to approximately the target value  $tr_{target}$ .

its elements:

$$\bigvee S = ((C_1 \vee C_2) \vee C_3) \vee \dots C_{|S|} \quad (2.4)$$

Any aperture adaptations of the resulting  $C_p^-$  as for the positive conceptors did not improve testing accuracy.

### 2.4.3 Testing

The combined evidence  $E$  was used to classify unforeseen speech samples via the corresponding ESN responses. The combined evidence  $E(x, p)$  that some state  $x$  corresponds to class  $p$  is a measure of similarity between that state and the positive and negative conceptors of class  $p$ . Concretely, it is the combination of a positive evidence  $E^+(x, p)$ , computed using the positive conceptor  $C_p^+$ , and a negative evidence  $E^-(x, p)$ , computed using the negative conceptor  $C_p^-$ :

$$\begin{aligned} E(x, p) &= E^+(x, p) + E^-(x, p), \\ E^+(x, p) &= x' C_p^+ x \\ E^-(x, p) &= x' C_p^- x \end{aligned} \quad (2.5)$$

$E(x, p)$  is large when  $x$  is close to the linear subspace modeled by conceptor  $C_p^+$ , but far from the linear

subspace which the other conceptors model (see definition of  $C_p^-$ ).

To classify a state  $x$ , the positive evidence is maximized over all classes:

$$\text{Class}'(x) = \arg \max_{p \in P} E(x, p) \quad (2.6)$$

**[Can I use self-explanatory names like Class' without explicitly stating what they are.]** To classify a point cloud  $X$  (a column-wise state collection matrix), the mean evidence for all states (columns of the collection matrix) is taken:

$$\text{Class}(X) = \arg \max_{p \in P} \frac{1}{L} \sum_{i=1}^L E(X[:, i], p), \quad (2.7)$$

where  $L$  is the width of  $X$ .

Finally, given a speech sample  $s_{new}$ ,  $\text{Class}(X_{new})$  returns the classification estimate, where  $X_{new} = [r(s_{new})(1)|\dots|r(s_{new})(L)]$  is the column-wise concatenation of the states collected when driving the ESN with  $s_{new}$  (excluding the starting state).

#### 2.4.4 Results

This testing procedure resulted in accuracies of 56.16% on the training set and 56.04% on the test set, both of which are significantly above chance  $100\%/|P| \approx 2,6\%$ . The confusion matrix in Figure A.1 of Appendix A shows the classification rates across the classes. For every phoneme, their rate of correct prediction (diagonal values) was higher than the rate of misclassification to any of other classes (off-diagonal values) suggesting an above-chance classification accuracy across all phonemic classes. Error rates seem to be elevated within phonetic groups like vowels (top left) and consonants (bottom right) [Potentially elaborate if necessary]. In an attempt to improve the accuracy, the experiment was repeated in slight adaptation to the type of data (Appendix A) which led to a training accuracy of 63.64% but test accuracy of 49.13. **[Is there anything else I need to report here?]**

## 2.5 Experiments 2 & 3: Conceptor-based Clustering

### 2.5.1 Introduction

In Experiment 1, an ESN setup (defined by its hyperparameters) was found that could effectively be

used to classify time-series. The same ESN states and similar conceptor-based mechanisms used during classification were subsequently reused as we **[We, I, or it?]** turned, in Experiments 2 and 3, to unsupervised methods for identifying meaningful symbols within ESN dynamics.

In the following two experiments, the traditional K-means and HAC algorithms were adapted and applied to cluster the ESN responses to the phonemic speech recordings. A theme in both experiments was to (A) embed time-series (the pre-processed phoneme recordings) as reverberations of an ESN. (B) Conceptors were then used to represent these ESN reverberations and (C) group them into a set of meaningful clusters. Figure 2.3 depicts the steps from the original signals to ESN states to conceptors to clusters. Although the conceptors were subjected to the clustering algorithms, the tight relationship between signals, ESN responses, and conceptors presumably allowed the resulting clusters to generalize from conceptors to the other two representations. This generalization was exploited during cluster evaluation when comparing the found clusters against phonetic groups of the TIMIT speech samples.

### 2.5.2 Experiment 2: Below-phoneme clustering

**Objective** blind the computer of any previously human-made symbols, the classes  $|P|$ , previously available during training, and attempt to determine a set of meaningful symbolic classes, tabula rasa **[Is this sentence too colloquial?]**. The following experiment aimed to group the pre-processed phoneme recordings into  $K$  clusters that coincided with the original phonemic classes. Four conditions resembling the K-means algorithm were used.

**Dataset** For computational constraints, only a subset  $D' \subset D_{train}$  of  $n' = 105$  samples was used for this experiment. To simplify the task while meeting the classical K-means assumption of equal-sized clusters,  $D'$  was constrained to 15 utterances of each of the phonemes in  $P' = \{/ih/, /ae/, /ah/, /iy/, /aa/, /eh/, /uh/\}$ . These phonemic classes were similar to those used in (Lerato and Niesler, 2012). Each utterance was sampled from a random subset of 48 speakers with an equal ratio across genders and dialect regions, a stratified sampling that ought to ensure an accurate representation of the population

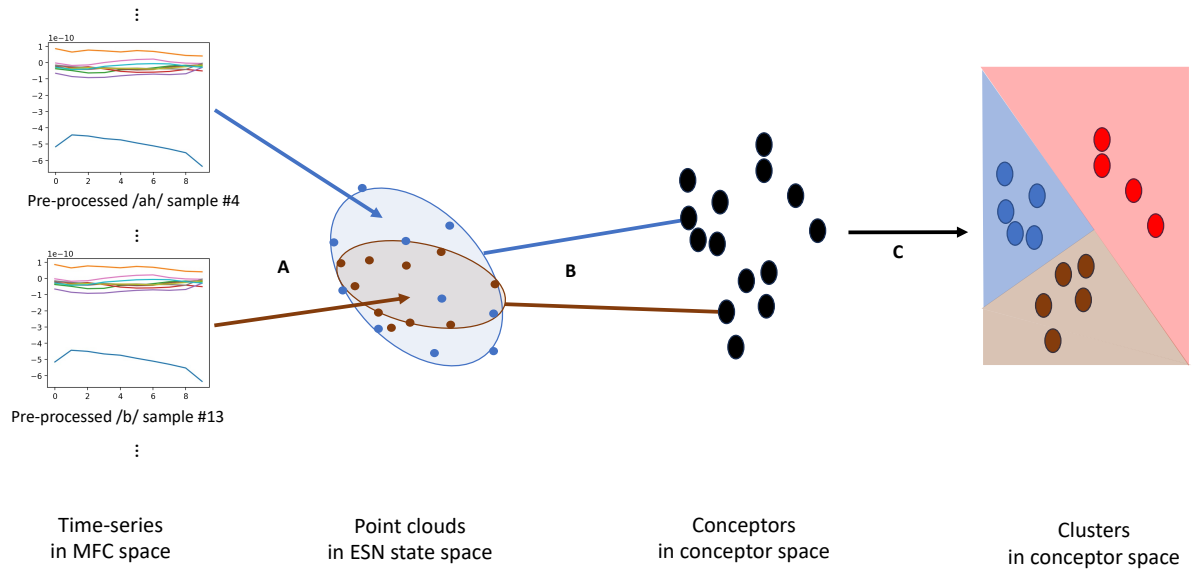


**Figure 2.3:** The steps from the MFC space of pre-processed speech signals to ESN state space by driving the ESN (A), followed by a transfer to conceptor space by computing conceptors (B), and finally the partitioning of the data into clusters (C). Note, while Experiment 2 aims to find partitions, Experiment 3 identifies hierarchies; thus, the right illustration would differ for Experiment 3. [Double check representation is truthful of apertures.]

and reduce potential bias. Moreover, only utterances from the phonetically compact sentences, which cover a wide range of phonemes in few contexts, were considered to limit phonetic variability.

**Conditions** The experiment was performed in four conditions – *MFCC-Euclidian*, *ESN-Euclidian*, *Conceptor-Evidence*, and *Mixed*. For each condition, K-means’ main components were customized as follows.

In the *Control* condition, the traditional version of K-means was implemented clustering the MFCC time series directly.

1. The set of points  $D'_{ctrl}$  contains the unlabeled MFCC time series from  $D'$ :

$$D'_{ctrl} = \{s^i | 0 < i \leq n'\} \quad (2.8)$$

2. Given a cluster  $Cl$ , its centroid is the mean of its members:

$$\text{centroid}_{ctrl}(Cl) = \frac{1}{|Cl|} \sum_{p^i \in Cl} p^i \quad (2.9)$$

3. The distance from point  $p^i$  to cluster  $Cl$  is the Euclidian distance between  $p^i$  and  $Cl$ ’s centroid:

$$d_{ctrl}(p^i, Cl) = ||p^i - \text{centroid}_{ctrl}(Cl)|| \quad (2.10)$$

In the *Conceptor* condition, an adaptation of K-means was implemented that uses conceptors as embeddings for the MFCC time series.

1. The set of points contains the conceptor embeddings of the MFCC time series in  $D'_{ctrl}$  and was computed as follows. A new ESN with the same hyperparameters as in Experiment 1 was driven independently with the MFCC time series  $s_i$  ( $0 < i \leq n'$ ). From each  $x_i$ , a conceptor  $C_i$  was derived, like in Experiment 1, with a preliminary aperture of 1 then to be adapted the value of 21.4 that maximized the gamma criterion among all conceptors  $C_i$ , and finally adapted to normalize the traces among the conceptors. We get the following the set of points:

$$D'_{con} = \{C_i | i = 1, \dots, n'\} \quad (2.11)$$

2. Given a cluster  $Cl$ , its centroid is the aperture-adapted disjunction of the cluster’s members:

$$\begin{aligned} \text{centroid}_{con}(Cl) &= \psi(\bigvee Cl, tr_D^-, 0.01), \\ \text{where } tr_D^- &= \frac{1}{|D|} \sum_{C \in D} \text{tr}(C) \end{aligned} \quad (2.12)$$

Alternatively, the conceptor centroid  $\text{centroid}_{con}(Cl)$  could be computed from the set of ESN responses that underlie the members of  $Cl$ , i.e., applying Procedure 1.5.2 to  $\{r(s_i) | i = 1, \dots, n'\}$  with an aperture of 1. With either approach, conceptor disjunction or recomputation, the resulting conceptor needed to be aperture-adapted to match the mean trace of the points in  $D'_{con}$  using Algorithm 2.1. Although the above computations would produce the same conceptor, the latter was used for being computationally cheaper.

3. The distance from point  $p$  to cluster  $Cl$  is the complement with respect to 1 of the conceptor similarity of  $p$  and  $Cl$ ’s centroid:

$$d_{con}(p, Cl) = 1 - \text{Sim}(p, \text{centroid}_{ctrl}(Cl)) \quad (2.13)$$

The ranges of  $d_{con}$  and  $\text{Sim}$  are  $[0, 1]$ , and smaller values of  $d_{con}$  indicate a higher degree of similarity between point  $p$  and the centroid of cluster  $Cl$ . **[Big problem: Not a Bregman divergence, because cosine similarity does not fulfill the triangle inequality. Therefore, this algorithm is not guaranteed to converge.]**

With these components set up for both conditions, hard clustering was performed. Thus, for each condition, its components (1,2,3) were substituted in the designated places of the generalized K-means algorithm. This algorithm uses the same iterative relocation scheme of K-means, but with additional input parameters for the centroid computation function and dissimilarity (distance) function.

The centroids were initialized in a K-means++ fashion. With this method, the initial centroids are sampled from a distribution that aims to spread them evenly across the point space. Compared to the random centroid-initialization of classical K-means, this method tends to converge faster and more consistently [cite AI2].

---

**Algorithm 2.2** Generalized K-means clustering algorithm. The numbers in brackets indicate the condition-specific components.

---

**Require:**

- Number of clusters  $K$
- [1] Set of points  $D = \{p_1, p_2, \dots, p_n\}$
- [2] Centroid computation function  $\text{centroid}(Cl)$
- [3] Dissimilarity function  $d(p_i, p_j)$

Initialize  $K$  cluster centroids via procedure 2.3:  
 $\mu = \{\mu_1, \mu_2, \dots, \mu_K\}$

**while** TRUE **do**

Reset all clusters:  $Cl = \{\emptyset, \emptyset, \dots, \emptyset\}$

Assignment step:

**for**  $p_i$  in  $D$  **do**

$k \leftarrow \arg \min_{1 \leq j \leq K} d(p_i, \mu_j)$

Assign  $p_i$  to cluster  $k$ :  $Cl_k \leftarrow Cl_k \cup p_i$

**end for**

Centroid update step:

**for**  $j = 1$  to  $K$  **do**

$\mu_j \leftarrow \text{centroid}(Cl_j)$

**end for**

**if** cluster assignments did not change **then**  
break because converged

**end if**

**end while**

**return** Set of clusters  $Cl = Cl_1, Cl_2, \dots, Cl_K$

---



---

**Algorithm 2.3** K-means++ improved initialization of centroids.

---

**Require:**

- Number of clusters  $K$
- Set of points  $D = \{p_1, p_2, \dots, p_n\}$
- Dissimilarity function  $d(p_i, p_j)$

Choose first centroid  $\mu_1$  uniformly at random from  $D$

**for**  $k = 2$  to  $K$  **do**

For each point  $p_i$ , compute distance to nearest centroid\*\*:

$$d_{min}(p_i) = \min_{0 < j < k} d(p_i, \mu_j)^2$$

Choose  $p_i \in D$  as the next centroid  $\mu_k$  with

$$\text{probability } \frac{d_{min}(p_i)}{\sum_{j=1}^n d_{min}(p_j)}$$

**end for**

**return** Set of centroids  $\mu = \{\mu_1, \mu_2, \dots, \mu_K\}$

---

**Evaluation** The resulting clusters were evaluated using one intrinsic measure [the mean intra-cluster dissimilarity (MICD)], and two extrinsic measures [the normalized mutual information (NMI) and classification accuracy].

First, the MICD is the mean dissimilarity between the clusters' centroids and member points. It is a measure of cluster cohesion, i.e., of how *tight* the clusters are, which translates to the crispness of the resulting symbols. Moreover, it resembles the optimization objectives of the original and adapted K-means algorithm, and a downward trend of the MICD over the iterations is expected. Thus, it was applied to inform about cluster cohesion and the convergence behavior of the algorithm.  $d_{Conceptor}$  being not a metric, it does not fulfill the assumptions of many alternative intrinsic cluster quality measures like the within-cluster sum of squares or the silhouette coefficient. Importantly, the values of the MICD are not comparable between conditions, since different dissimilarity functions and data were used. Given a clustering  $Cl = \{Cl_1, Cl_2, \dots, Cl_K\}$ , where  $Cl_k$  is the set of points assigned to cluster  $k$ , the MICD is calculated as follows. For any cluster  $Cl_k$ , let the intra-cluster dissimilarity (ICD) be the mean dissimilarity between its member points  $p_i$

and its centroid  $\text{centroid}(Cl_k)$  :

$$ICD(Cl_k) = \frac{1}{|Cl_k|} \sum_{p_i \in Cl_k} d(p_i, \text{centroid}(Cl_k)) \quad (2.14)$$

where  $d(p_i, \text{centroid}(Cl_k))$  is the dissimilarity function and depends on the condition. The MICD is then the mean of the ICD values for all clusters:

$$MICD = \frac{1}{K} \sum_{k=1}^K ICD(Cl_k) \quad (2.15)$$

where  $K$  is the number of clusters.

Second, the NMI is an extrinsic measure of the similarity between a clustering  $Cl = \{Cl_1, Cl_2, \dots, Cl_K\}$ , where  $Cl_k$  is the set of points assigned to cluster  $k$ , and the ground-truth phonemic groups  $G = \{G_1, G_2, \dots, G_{|P'|}\}$ , where  $G_p$  is the set of points with label  $p$  in the dataset  $D'$ . Its values range from 0 for completely dissimilar clusterings and 1 for identical clusterings. It was used to compare the empirically found clusters with the phonemic classes of TIMIT. To compute the NMI, the mutual (shared) information  $I$  between  $Cl$  and  $G$  is normalized by the mean entropy (uncertainty)  $H$  within each clustering:

$$\begin{aligned} I(G, Cl) &= \sum_{G_p \in G} \sum_{Cl_k \in Cl} P(G_p \cap Cl_k) \log \frac{P(G_p \cap Cl_k)}{P(G_p)P(Cl_k)} \\ H(G') &= - \sum_{G'_p \in G'} P(G'_p) \log P(G'_p), \text{ for some clustering } G' \\ NMI(G, Cl) &= \frac{I(G, Cl)}{\frac{1}{2}[H(G) + H(Cl)]} \end{aligned} \quad (2.16)$$

Third, I evaluated how accurately the conceptors derived from the clusters could classify new phonemes. This extrinsic measure, that I will refer to as *cluster classification accuracy* (CCA), ought to measure how accurately the acquired symbols this system could be used to represent certain entities, phoneme utterances in this case. Therefore, it was assumed that each cluster corresponded, to different degrees, with one of the phonemic classes  $P$ . A greedy bijection of clusters and classes was made by iteratively matching the remaining cluster

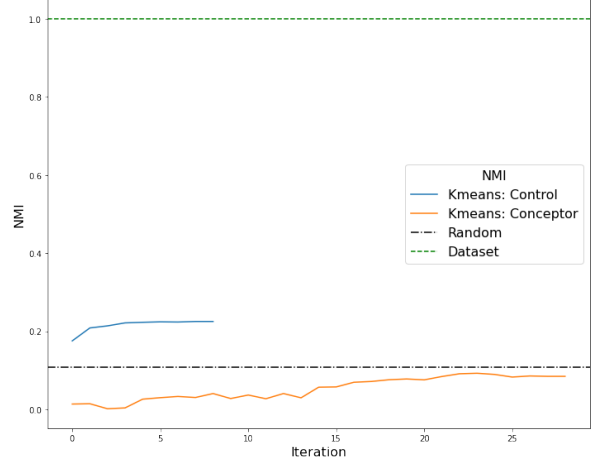


**Figure 2.4: The NMIs of the clusterings throughout the iterations of an example run with  $K = |P'|$ . Comparison to the NMI of randomly initialized clusters and clusters equal to the TIMIT classes.**

and class with the greatest intersection. Then, using the clusters and matched labels, Experiment 1 was essentially replicated; the points in each cluster were used to train the conceptor-based classifier for the matched class. The classifier was tested on a set composed of the remaining 1759 phonetically diverse utterances of phonemes  $P'$  from the the eight selected speakers.

**Run** The experiment was run with the following settings. The numbers of clusters  $K$  was swepted from  $K = 1$  to  $K = 18$ . For each  $K$ , Algorithm 2.2 was repeatedly run on each condition for 20 trials to reduce the effects of randomness of the cluster initialization.

**Results** The MICDs, NMIs, and CCAs at each iteration, averaged across the trials, is shown in Figure ??.

Figures 2.4 and ?? show the evolution of the NMIs and SCs in the first of the two trials for  $K = |P'|$  and compare these results to randomly initialized clusters and to clusters of the dataset classes.

## 2.6 Experiment 3: Above-phoneme

The second clustering algorithm aimed to structure the conceptors  $C^+$  in a hierarchy through an adap-



tation of HAC. Whereas in Experiment 2, symbols were identified among ESN states grouped by utterance (a more concrete symbol), this experiment aims to identify symbols among ESN states grouped by phoneme (a more abstract symbol). Reiterating, symbols represent entities that themselves can be groups symbols. Indeed, many domains, like Phonetics, are conceptually structured as hierarchies or taxonomies of symbols of increasing levels of abstraction. This experiment is an attempt to distill such a symbolic abstraction hierarchy from a set of conceptors (one per phoneme) proxying for patterns among the corresponding ESN states.

**Method** The following three components were used to adapt traditional HAC to the clustering of conceptors:

1. The set of points to be clustered consisted of one conceptor embedding per phonemic class of the corresponding samples in the training set. Therefore, the set of positive conceptors from Experiment 1 was reused:

$$D_{HAC} = C^+ = \{C_p^+ | p \in P\} \quad (2.17)$$

2. The dissimilarity measure between points  $p_i$  and  $p_j$  was the negative logarithm of the conceptor similarity of  $p_i$  and  $p_j$ :

$$d(p_i, p_j) = 1 - \text{Sim}(p_i, p_j) \quad (2.18)$$

This function fulfils several desirable properties for a dissimilarity measure: It is non-negative, symmetric, and equals 0 for identical inputs.

3. The linkage function  $d_{link}(Cl_i, Cl_j)$  between clusters  $Cl_i$  and  $Cl_j$  is the mean pairwise dissimilarity of the points in the clusters. This is the defining function of *average* linkage algorithms:

$$\begin{aligned} d_{link}(Cl_i, Cl_j) \\ = \frac{1}{|Cl_i||Cl_j|} \sum_{p_x \in Cl_i, p_y \in Cl_j} d_{HAC}(p_x, p_y) \end{aligned} \quad (2.19)$$

From these components, the HAC adaptation was performed as detailed in Algorithm 2.4.

---

#### Algorithm 2.4 Generalized HAC

---

- [1] Set of points  $D = \{p_1, p_2, \dots, p_n\}$
- [2] Dissimilarity function  $d(p_i, p_j)$
- [3] Linkage function  $d_{link}(Cl_i, Cl_j)$

Initialize a cluster for each point:  $Cl \leftarrow D$

**while** number of clusters  $> 1$  **do**

Find the two most similar clusters:

$$Cl_i, Cl_j \leftarrow \arg \min_{Cl_i \neq Cl_j} d_{link}(Cl_i, Cl_j)$$

Update clusters in  $Cl$ :

Remove  $Cl_i$  and  $Cl_j$

Add  $Cl_{merged} = Cl_i \cup Cl_j$

**end while**

---

**Results** The resulting hierarchy is depicted as a dendrogram in Figure 2.5. Each leaf on the left represents a phonemic group. Moving toward the right, phoneme clusters emerge. The dissimilarities between merged child clusters is the abscissa of their link.

Several overlaps can be identified between the HAC phoneme clustering results and phonetic groups depending on the choice of phonetic model. We will compare the clusters with the classes provided by Pfeifer and Balik (2011) and shown in Figure 1.2, for their model is based on manner of production that seems the variable most correlated to the HAC clusters. Table 2.1 depicts these overlaps with the phonetic groups in the left column and their associated phonemes in the right column. Each group also corresponds to an HAC cluster with the exception of some **bold** phonemes that were moved between sibling clusters. The two primary clusters encompass consonants and vowels with a dissimilarity of about 0.015. Within the upper, consonants, cluster five subgroups can be identified. The red subcluster corresponds to fricatives and affricates (enclosed), both produced with air friction. The green subcluster encompasses plosives (top) and nasals (bottom). However, instead of the manner of production, the place of production may be considered as the group-determining variable. Thus, several other overlaps of the subclusters of consonants with phonetic groups may be found; the *bilabial* stops /p/ and /b/, the *alveolar* stops /t/ and /d/, the *velar* stops /k/ and /g/, and the *alveolar* fricatives /s/

Group	Phonemes of Group
Conso- nants	th f sh z s <b>dh v hh</b>
	jh ch
	p b d t g k <b>dx</b>
	m n ng
	ow aa oy ah uh er aw ay ey eh ae iy ih uw
Vowels	
Mixed	<b>l r w y</b>
Silence	h#

**Table 2.1: Linguistic groups found within the phoneme clusters that resulted from HAC.**

and /z/ were each assigned to exclusive subclusters.

The lower cluster predominantly consists of vowel sounds. No significant correspondence between the sub-clusters of vowels and their pronunciation position or other articulatory features is apparent.

The phonemes in the Mixed group are considered separately, for their articulatory features resemble both vowels and consonants. The group contains the liquids /l/ and /r/ and semivowels /w/ and /y/. These instances all needed to be moved, since no cluster exclusively corresponded to the mixed group. Lastly, the silence /h#/ is considered separately like by Pfeifer and Balik (2011).

In summary, the table displays how the organization of phonemes derived from HAC coincides with traditional phonetic categories. The large resemblance suggests that the HAC algorithm produced meaningful and mostly coherent clusters.

### 3 Discussion

**Exp 1: Phoneme Classification** Experiment 1 demonstrated phoneme classification using conceptors. [Comparison to phoneme classification benchmark...] [Comparison to Jaeger’s experiments...]

**Aperture normalization** The methods of conceptor based time series classification used in Ex-

periment 1 were largely inspired by (Jaeger, 2014) with the exception of the aperture adaptation. The first deviation here was to adapt explicitly only the apertures of the positive conceptors  $C^+$ ..... **[normalizing/optimizing the aperture of the negative conceptors does not help]** It was made to avoid to give conceptors with larger singular values an advantage during classification. To understand this effect, consider the example of a  $2 \times 2$  conceptor matrix  $A$ . [...] To avoid such classification errors, the apertures were iteratively adapted until approaching a target singular value sum using the following procedure. Indeed this normalization further improved classification.

It must be remarked that, by that process, the final apertures will deviate from the one originally chosen aperture via the  $\nabla$ -criterion. Figure 2.2 depicts this normalization process for the classification experiment.

**Dataset** Without normalization in time, performance decreases. How to handle different utterance speeds? Add leakiness to ESN to integrate time scales? Non-stationary signals

**Z-Condition** Worse due to overfitting: Exponential reason (AI2). The size of  $z$  and the associated computational costs are larger than for the former method, and it tends to lead to better *training* classification accuracy, but much worse test accuracy indicating overfitting.

**Exp 2: Advantages of clustering method** Conceptors do not [...]. As constant-sized matrices, they do not scale with the number of time steps or modeled states. This is a leap for analyzing time series since previous algorithms typically scale poorly with longer samples; for example, computing the distance between time series in dynamic time warping (DTW) scales quadratically with sample length dynamic. Notwithstanding, the quality of conceptors depends on the number of states used for their computation [...]. [Comparing responses of different lengths would require workarounds like Dynamic Time Warping (DTW).]

Third, ESNs deal with time-extended inputs causing several difficulties for preexisting clustering algorithms. For example, the euclidian distance can

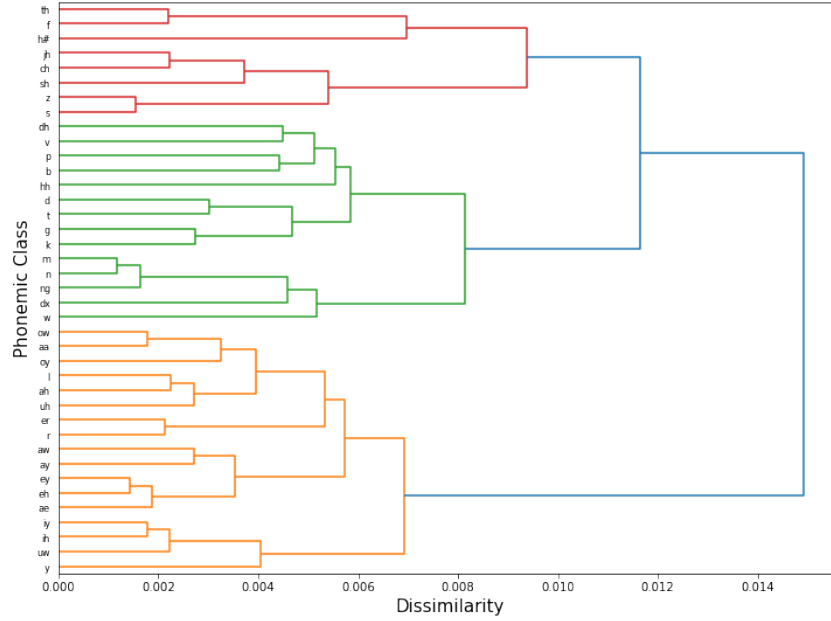


**Figure 2.5:** Dendrogram of the hierarchy that resulted from the adapted average linkage agglomerative clustering algorithm.

only be used to compare samples of different durations (for clustering algorithms that require distance functions) and have time-.

[Time complexity of clustering algorithms: especially Experiment 2]

[Mention esp might not be satisfied]

[Effects of spectral radius on ESP]

It should be stressed that, in the current work, *ESN activities* are classified and clustered using conceptors; Not speech signals, but an ESN's responses to these signals are used as input to classification and clustering algorithms.

**Applications** BPTT: To evaluate how well a classifier can distinguish between a set of classes, one may resort to performance metrics or investigate the degree of certainty in its predictions. However, such an evaluation relies only on the outputs and disregards the internal states that led to the predictions. For complex models or whole pipelines, it may be of interest to find groups or clusters present in the RNN's activations or within a subset thereof, e.g., corresponding to only one part of a pipeline. This study ought to be an exploratory step toward answering the following questions: How clustered are

the activities within a NN? When, during training, do class differences in network activities arise?

Nonetheless, a phonetic interpretation about the speech signals will be made which, however, requires an assumption. Commonly, the echo state property is used to ensure a functional relationship between driver signal (phoneme recording) and RNN response Yildiz et al. (2012). However, for the echo state to be reached requires left-infinite or at least considerably long input sequences, for the starting state to be washed out. In our case, inputs will be downsampled to a length of 10 rendering the claim of the ESP impossible based on current theory. The analyzed states will most likely still correspond to the network's initial transient period. Thus, functionality between input and response cannot be guaranteed but only assumed. Hence, we shall nonetheless use the results of clustering and classification of ESN activities from the transient period for an interpretation about the input signals.

The current algorithm is not guaranteed to converge since it is an adaptation of K-Means that uses a non-Bregman divergence function (more on this in the comment under Experiment 2).

Adv of conceptor-based clustering to classical:

Moreover, they compress one or more network states into a mathematical object (a matrix). These are other advantages. This hurdle can be met and one advantage of applying conceptors to time series is, as will be further argued, that they capture their information in a static mathematical compression of the temporal dimension and

To summarize, the three main motivations of the following clustering methods are to provide additional.

1. Explainability: Clustering RNN dynamics could help explain what groups of activity are present in the network. For example, both algorithms could be helpful tools for interpreting BPTT-trained RNNs. For example, Experiment 2 could show how classes become more distinct or numerous within the RNN (form activity clusters) while training.
2. Data analysis: Clustering time series with traditional clustering algorithms can be challenging. For instance, due to varying input lengths, methods for embedding time-series data are rather limited (e.g., latent-space encodings). This paper shows that the clusters present in RNN dynamics can be tied back to clusters within the inputs used to produce these dynamics.
3. Conceptor Classification: To the end of successful clustering, a phoneme classification experiment (Experiment 1) will be performed. In this experiment, the current methods for conceptor-based classification are applied and extended.

**Conceptors as state Embeddings** The temporal and spatial compression realized by conceptors, allows them to be used as embeddings of ESN responses. Unifying responses in conceptor-space, independently of their length and maintaining only their most important information, allows state sequences to be related and compared. [Examples of the use of conceptors as embeddings]

Classically, these algorithms are used on data in Euclidian space and their components are well-defined for that space (mean, Euclidian distance, manhattan distance, etc.). However, the activities

within the ESN are subjected to non-linear transformations like *tanh* at each time step as is the case for most neural networks. I hypothesize that Euclidian distance functions may not be well-suited to capturing the distances between network states. Moving to conceptor space will be an attempt to improve the clustering of ESN activities through a more adequate means for cluster representation, comparison, and assignment.

Finally, one may object that, for unsupervised symbol acquisition, the use of hard clustering is very artificial and something akin to Hebbian learning should be preferred, something that resembles how the brain acquires symbols. However, often in computing, and especially reservoir computing for material constraints, learning may not be possible. Yet, one may want to identify the symbols prevalent in the "artificial mind".

... We attempt to solve this mismatch by mapping the network states to be clustered to conceptors since conceptors offer several tools for comparing and analyzing network states. By moving to conceptor space, the following adaptations were made.

1. plus becomes or: Firstly, the operations of Euclidian vector space were changed.
2. division become aperture adaptation
3. Distance becomes the one proposed by Jaeger (2014) OR...

Problems. Distance metric is rather unclear, lack of semantics. Average linkage: Linkage algorithms: Pros and Cons slide of video

Categories may be due to coarticulation / correlations

## 4 Conclusions

Conceptors are well-suited to apply clustering algorithms to time-series and ESN dynamics.

## References

Arindam Banerjee, Srujana Merugu, Inderjit S Dhillon, Joydeep Ghosh, and John Lafferty. Clustering with bregman divergences. *Journal of machine learning research*, 6(10), 2005.

- Margaret A Boden. *The creative mind: Myths and mechanisms*. Psychology Press, 2004.
- Paul Bricman, Dr Herbert Jaeger, and Dr Jacolien van Rij-Tange. Nested state clouds: Distilling knowledge graphs from contextual embeddings. Bachelor’s thesis, University of Groningen, 8 2022.
- William G Chase and Herbert A Simon. Perception in chess. *Cognitive psychology*, 4(1):55–81, 1973.
- Satchit Chatterji. Cut the carp! using context to disambiguate similar signals using conceptors. Bachelor’s thesis, University of Groningen, 8 2022.
- Peter I Frazier. A tutorial on bayesian optimization. *arXiv preprint arXiv:1807.02811*, 2018.
- Herbert Jaeger. Controlling recurrent neural networks by conceptors. *arXiv preprint arXiv:1403.3369*, 2014.
- Herbert Jaeger, Mantas Lukoševičius, Dan Popovici, and Udo Siewert. Optimization and applications of echo state networks with leaky-integrator neurons. *Neural networks*, 20(3):335–352, 2007.
- Peter Karsmakers, Kristiaan Pelckmans, Johan AK Suykens, and Hugo Van hamme. Fixed-size kernel logistic regression for phoneme classification. In *INTERSPEECH*, pages 78–81, 2007.
- K-F Lee and H-W Hon. Speaker-independent phone recognition using hidden markov models. *IEEE Transactions on Acoustics, Speech, and Signal Processing*, 37(11):1641–1648, 1989.
- Lerato Lerato and Thomas Niesler. Investigating parameters for unsupervised clustering of speech segments using timit. In *Twenty-Third Annual Symposium of the Pattern Recognition Association of South Africa*, page 83, 2012.
- Carla Lopes and Fernando Perdigao. Phoneme recognition on the timit database. In Ivo Ipsić, editor, *Speech Technologies*, chapter 14. IntechOpen, Rijeka, 2011. doi: 10.5772/17600. URL <https://doi.org/10.5772/17600>.
- Mantas Lukoševičius. A practical guide to applying echo state networks. *Neural Networks: Tricks of the Trade: Second Edition*, pages 659–686, 2012.
- Jessica Maye and LouAnn Gerken. Learning phonemes without minimal pairs. In *Proceedings of the 24th annual Boston university conference on language development*, volume 2, pages 522–533, 2000.
- Brian McFee, Colin Raffel, Dawen Liang, Daniel Ellis, Matt McVicar, Eric Battenberg, and Oriol Nieto. librosa: Audio and music signal analysis in python. pages 18–24, 01 2015. doi: 10.25080/Majora-7b98e3ed-003.
- George A Miller. The magical number seven, plus or minus two: Some limits on our capacity for processing information. *Psychological review*, 63(2):81, 1956.
- Till Mossakowski, Razvan Diaconescu, and Martin Glaue. Towards fuzzy neural conceptors. *IfCoLog Journal of Logics and their Applications*, 6(4):725–744, 2019. URL <https://collepublications.co.uk/ifcolog/?00033>.
- Allen Newell and Herbert A Simon. Computer science as empirical inquiry: Symbols and search. In *ACM Turing award lectures*. 1975.
- Vaclav Pfeifer and Miroslav Balik. Comparison of current frame-based phoneme classifiers. *Advances in Electrical and Electronic Engineering*, 9, 12 2011. doi: 10.15598/aeec.v9i5.545.
- Jamie Vlegels. Multivariate time series classification using conceptors: Exploring methods using astronomical object data. Bachelor’s thesis, University of Groningen, 2022.
- Izzet B Yildiz, Herbert Jaeger, and Stefan J Kiebel. Re-visiting the echo state property. *Neural networks*, 35:1–9, 2012.

## A Appendix

### A.1 Computing Projector Matrix

The following algorithm for computing projector matrix  $P_{R(C) \cap R(B)}$  is taken from Jaeger (2014).  $C$  and  $B$  are conceptors of size  $N$ . We begin by computing the basis matrix  $B_{R(C) \cap R(B)}$  as follows:

1. Compute the SVDs  
 $C = U \text{diag}(s_1, \dots, s_l, s_{l+1}, \dots, s_N) U'$  and  
 $B = V \text{diag}(t_1, \dots, t_m, t_{m+1}, \dots, t_N) V'$ , where  $l$  and  $m$  are the indices of the last singular values if  $C$  and  $B$  not below the arbitrary threshold  $\epsilon_{impr} = 10^{-10} \approx 0$ ; This approximation is to account for computational imprecision [**Is this the right word?**], but in theory,  $s_{l+1}, \dots, s_N$  and  $t_{m+1}, \dots, t_N$  should all equal to 0.
2. Let  $U_{>l}$  be the submatrix of  $U$  made from the last  $N - l$  columns of  $U$ , and similarly, let  $V_{>m}$  consist of the last  $N - m$  columns of  $V$ .
3. Compute the SVD  
 $U_{>l}(U_{>l})' + V_{>m}(V_{>m})' = W \Sigma W'$ , where  
 $\Sigma = \text{diag}(\sigma_1, \dots, \sigma_k, \sigma_{k+1}, \dots, \sigma_N)$ . Again,  $k$  is the index of the last singular value of  $C$  not below  $\epsilon_{impr}$ .
4.  $B_{R(C) \cap R(B)} = W_{>k}$ , the submatrix of  $W$  consisting of the last  $N - k$  columns of  $W$ .

Finally,  $P_{R(C) \cap R(B)} = B_{R(C) \cap R(B)} B'_{R(C) \cap R(B)}$ .

### A.2 Dataset

Table A.1 lists the phone classes and their frequencies within the processed TIMIT dataset.

### A.3 Additional Results of Experiment 1

Figures A.2 and A.3 relate the number of clusters to cluster quality as measured by the NMI and the SC scores, respectively.

### A.4 Extension of Experiment 1: Hyperparameter Optimization

Hyperparameters  $k_b, k_{W^{in}}, r$  and  $\rho$  were also tuned automatically using bayesian optimization procedure of the Bayesian Optimization python package. The optimization objective was to maximize

Phone	Folded	#Training	#Test
iy		6953	2710
ih	ix	13693	4654
eh		3853	1440
ae		3997	1407
ah	ax-h ax	6291	2343
uw	ux	2463	750
uh		535	221
aa	ao	6004	2289
ey		2282	806
ay		2390	852
oy		684	263
aw		729	216
ow		2136	777
l	el	6752	2699
r		6539	2525
y		1715	634
w		3140	1239
er	axr	5453	2183
m	em	4027	1573
n	en nx	8762	3112
ng	eng	1368	419
ch		822	259
jh		1209	372
dh		2826	1053
b		2181	886
d		3548	1245
dx		2709	940
g		2017	755
p		2588	957
t		4364	1535
k		4874	1614
z		3773	1273
v		1994	710
f		2216	912
th		751	267
s		7475	2639
sh	zh	2389	870
hh	hv	2111	725
h# (silence)	dcl tcl kcl bcl pcl pau epi q gcl	39467	14021
$\Sigma$	39 22	177080	64145

Table A.1: Phone labels and their frequencies. Column 1: Phone classes. Column 2: Phones that were originally present in TIMIT but folded into a class with the left-adjacent phone. Columns 3 & 4: Number of speech samples of each class. Bottom row: Sums of classes or samples.

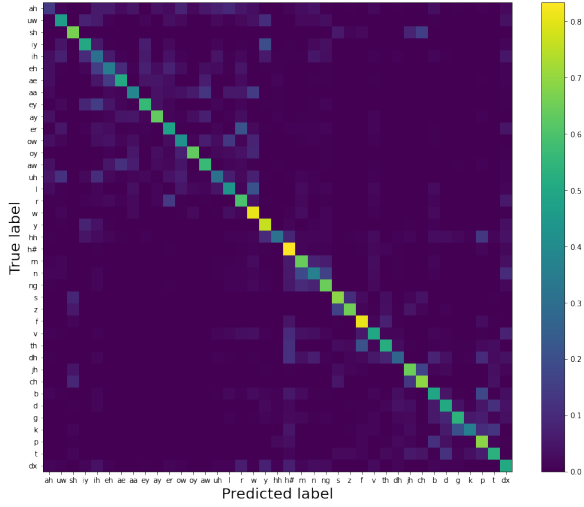


Figure A.1

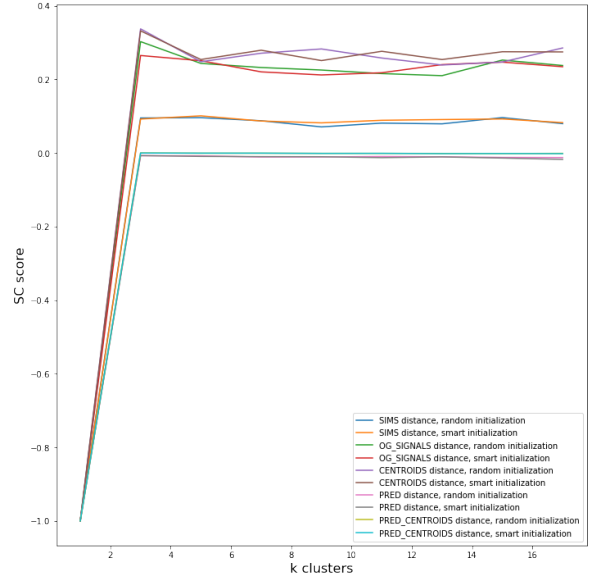


Figure A.3: SC scores by values of  $k$  across conditions

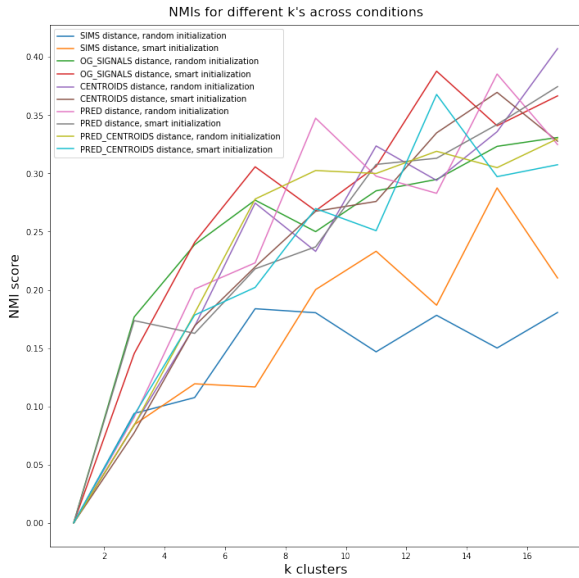
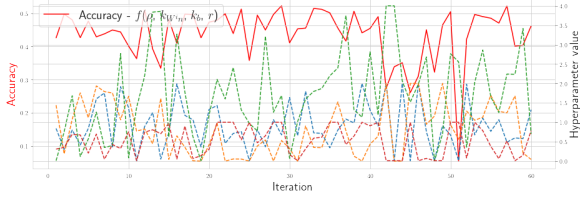


Figure A.2: NMI scores by values of  $k$  across conditions

the testing accuracy of phoneme classification in Experiment 1. Concretely, after 10 initial exploration steps, 40 optimization steps were taken. At each optimization step, a set of hyperparameters is sampled from a promising region of the hyperparameter space trying to maximize an estimated surrogate  $\bar{f}$  for the unknown objective function  $f[f(\rho, k_{Win}, k_b, r) := \text{accuracy}]$ . After training and testing the phoneme classifier with these hyperparameters on the training set (with a train-test split), the surrogate estimate is improved (for a detailed review of bayesian optimization, see Frazier). The hyperparameter space was restricted to:

- bias scaling parameter  $b \in (0, 2)$
- input weight scaling parameter  $k_{Win} \in (0.01, 0.99)$
- spectral radius  $r \in (0.01, 4)$
- internal weight density  $\rho \in (0.01, 1)\%$

The progress of the bayesian optimizer is depicted in Figure A.4. Bayesian optimization was preferred over the more straightforward grid search, since, under consideration of the high computational complexity of training the classifier (about 30 minutes



**Figure A.4: Hyperparameter tuning with the bayesian optimizer and accuracy [Still no progress seems to occur. This experiment will need to be repeated.]**

density of  $r' = 10\%$  was used. Scaling factors were changed to  $k'_{Win} = 1.5$  and  $k'_b = 0.2$ . A spectral radius of  $\rho' = 1.5$  was used. A training accuracy of 63.64% and test accuracy of 49.13 were reached.

on my computer), the reduced number of training steps outweighed the overhead added by the bayesian optimizer.

## A.5 Extension of Experiment 1: Inclusion of input states

Experiment 1 was repeated in slight adaptation of its methods to the stationary type of data. Jaeger (2014) demonstrated that conceptors may be used to classify signals produced by stationary and non-stationary processes. Stationary processes produce the same kind of signal (with the same probability distribution) over time; for example, white noise or sin waves are the results of stationary processes. Meanwhile, non-stationary processes change their properties over time leading to signals like speech whose probability distributions change over time. Meanwhile in the current classification method, the order within a sequence of states does not affect the resulting conceceptor since it is lost when computing the correlation matrix. This works fine on signals from stationary sources where temporal order is of no relevance. However, for non-stationary sources, states can have different probabilities of occurring depending on their position in the sequence, information not accounted for in the current classification method. Jaeger (2014) approached this limitation by unrolling the ESN response  $x(n)_n = 1, \dots, L$  into a vector  $z$  reserving a dimension for each step in time. Moreover, the input signal  $s$  is appended to  $z$  for additional information. We have  $z = [x(0); s(0); x(1); s(1); \dots; x(L); s(L)]$ . For  $z$ , the same classification procedure applies. New hyperparameters were picked by hand; the ESN size was reduced to  $N' = 40$  neurons due to the larger computational complexity of this method, but the same



## B Appendix

### B.1 Mathematical notations

Notation	Meaning
$A'$ or $x'$	Transposes of matrix $A$ or vector $x$
$I$	$N \times N$ identity matrix, $N$ to be inferred from context
$[x y]$	Matrix resulting from the column-wise concatenation of vectors $x$ and $y$
$[x;y]$	Matrix resulting from the row-wise concatenation of vectors $x$ and $y$
$A[:, y]$	Vector corresponding to the $y$ 'th column of matrix $A$
$A[x, :]$	Vector corresponding to the $x$ 'th row of matrix $A$
$ S $	Cardinality of set $S$
$\ A\ $	Frobenius norm of matrix $A$
$\text{diag}(A)$	Vector containing the main diagonal of matrix $A$
$ x $	Magnitude of vector $x$
$A^\dagger$	Pseudo-inverse of square matrix $A$
$R(A)$	Range of matrix $A$
$\text{tr}(A)$	Trace of square matrix $A$
$P_S$	$N \times N$ Projector matrix on the linear subspace $S$ of $\mathbb{R}^N$ , $N$ to be inferred from context
$S \cap Z$	Intersection of linear spaces $S$ and $Z$

**Table B.1:** List of some of the mathematical notations used throughout the paper.